



**HAL**  
open science

# Preparation condition, composition and post-preparation thermal treatment assisted control of structural and magnetic properties of spinel nano ferrites

Shashank Kane, Rulan Verma, Priyanka Tiwari, Frédéric Mazaleyrat

## ► To cite this version:

Shashank Kane, Rulan Verma, Priyanka Tiwari, Frédéric Mazaleyrat. Preparation condition, composition and post-preparation thermal treatment assisted control of structural and magnetic properties of spinel nano ferrites. *Advances in basic Science (ICABS 2019)*, Feb 2019, Bahal, India. pp.020003, 10.1063/1.5122326 . hal-04452984

**HAL Id: hal-04452984**

**<https://hal.science/hal-04452984>**

Submitted on 12 Feb 2024

**HAL** is a multi-disciplinary open access archive for the deposit and dissemination of scientific research documents, whether they are published or not. The documents may come from teaching and research institutions in France or abroad, or from public or private research centers.

L'archive ouverte pluridisciplinaire **HAL**, est destinée au dépôt et à la diffusion de documents scientifiques de niveau recherche, publiés ou non, émanant des établissements d'enseignement et de recherche français ou étrangers, des laboratoires publics ou privés.

Copyright

RESEARCH ARTICLE | AUGUST 29 2019

# Preparation condition, composition and post-preparation thermal treatment assisted control of structural and magnetic properties of spinel nano ferrites

S. N. Kane ; R. Verma; P. Tiwari; F. Mazaleyrat

 Check for updates

AIP Conf. Proc. 2142, 020003 (2019)

<https://doi.org/10.1063/1.5122326>



CrossMark



Cut Hall measurement time in *half* using an M91 FastHall™ controller



Also available as part of a tabletop system and an option for your PPMS® system

# Preparation condition, composition and post-preparation thermal treatment assisted control of structural and magnetic properties of spinel nano ferrites

S. N. Kane<sup>1, a)</sup>, R. Verma<sup>1</sup>, P. Tiwari<sup>1,2</sup> and F. Mazaleyrat<sup>3</sup>

<sup>1</sup>Magnetic Materials Laboratory, School of Physics, D. A. University, Khandwa road, Indore – 452001, India.

<sup>2</sup>Department of Physics, Prestige Institute of Engineering Management and Research, Indore - 452010, India.

<sup>3</sup>SATIE, ENS Universite Paris-Saclay, CNRS 8029, 61 Av. du Pdt. Wilson, F-94230, Cachan, France.

<sup>a)</sup>Corresponding author: kane\_sn@yahoo.com

**Abstract.** Study of ferrites has always been a topic of immense significance from the point of view of their magnetic applications, including their usage in high frequency devices, microwave devices, bioscience. For the same, there is a need to understand magnetic properties, and their correlation with structural properties, to be able to have a suitable material for a specific application. This article reviews various spinel ferrite systems in the framework of a specific synthesis protocol (*with variable synthesis parameters, including microwave assisted green synthesis etc.*), a precise composition (*with possibilities for its modification*), and usage of post-preparation thermal treatment (e. g. - conventional furnace annealing, microwave sintering, park plasma sintering, ion irradiation etc.). Complimentary information on structural (by x-ray diffraction 'XRD'); magnetic (by vibration sample magnetometer 'VSM') properties as well are described. Representative examples of ferrite nano particles are also given, depicting the effect of composition, synthesis protocol, and post-preparation treatment (*including an overview of various spinel nanoparticles in tabular form*), showing modification of structural, magnetic properties, correlation between them is illustrated.

## INTRODUCTION

### *About Ferrites*

Ferrites are technologically important ceramic materials that have been widely used in various applications (in high frequency devices, microwave devices, bioscience ) and, understanding the origin of the magnetic order is essential for the development of new technological strategies to design materials suitable for spintronics applications. Spinel ferrites have a general formula  $Me^{2+}O.Fe^{3+}_2O_3$  (where Me represent divalent ions  $Mg^{2+}$ ,  $Zn^{2+}$ ,  $Ni^{2+}$  etc.), are technologically important owing to their interesting structural, magnetic properties [1]. Spinel ferrites show ferrimagnetism, display face centered cubic (fcc) structure belongs to space group  $Fd_3m$ , having two interpenetrating sub-lattices A (*tetrahedrally coordinated, and occupied by divalent metal ions  $Me^{2+}$* ), and B (*octahedrally coordinated and occupied by trivalent ion  $Fe^{3+}$* ) [2]. Tuning structure (via control on structural parameters e. g. - average grain diameter, lattice parameter, density, etc.) of ferrites can be achieved by: i) **a specific synthesis protocol** (*with variable synthesis parameters*) [3], ii) **a particular ferrite composition** (*with possibilities for its modification*) [4], and iii) **an explicit post-preparation thermal treatment** (e. g. - conventional furnace annealing, microwave sintering, park plasma sintering, ion irradiation etc.) [5-8] etc., and can play a decisive role to have precise control on magnetic properties.

### *About effect of particle size*

Magnetic properties are quite susceptible to particle size, determined by finite dimension effects, is related to the reduced number of spins cooperatively linked within the particle, and by surface effects, which become more, and more important as the particle size decreases (1 – 100 nm) [9]. Under reduced particle size, the properties of nano-materials differ from the properties of their bulk counterparts in spite of the fact that they possess the same chemical

composition. Larger surface to volume ratio (*develops a substantial proportion of atoms having a different magnetic coupling with neighboring atoms, leading to differing magnetic properties*), and quantum effects are the two important principle factors of nanomaterials which cause the structural, optical, electrical, and magnetic properties of nano-materials to differ significantly from bulk materials. Large surface area to volume ratio in magnetic materials develops a substantial proportion of atoms having a different magnetic coupling with neighboring atoms, leading to differing magnetic properties. The ability to control the material properties by changing its surface area is important in many technological applications [10, 11]. Super-paramagnetism is observed in magnetic nano-particles, where the magnetization of the particles is randomly oriented, and can be aligned only under an applied magnetic field, and it vanishes upon removal of the magnetic field. This is due to the presence of single-domain in magnetic nanoparticles in contrast to multi-domains in the bulk material.

## PREPARATION TECHNIQUES

A specific synthesis technique, and a particular composition e. g. - [12 and references there-in] can be used to effectively control the properties of ferrites. In this context sol-gel auto combustion has emerged as one of the most efficient methods (utilizes conventional fuel e. g. - citric acid etc.), for preparing nano materials under moderate conditions e. g. – their preparation at relatively lower temperature  $\sim 90$  °C (*usually generated by conventional heating methods e. g. - via heating elements*), allowing one to tune magnetic properties by selectively controlling the structure via sintering temperature [13]. It is of value to note that in sol gel auto combustion method the ferrite phase formation is observed even in dry gel form, where no sintering is needed, thus establishing this technique as an energy efficient synthesis protocol. Here sintering can be performed at relatively lower temperatures (  $\sim 500$  °C) resulting in the formation of nano-grains with increased surface area, which in turn will decrease the free energy during sintering, that remains the key driving force for lowering the sintering temperature. In sol-gel auto combustion method, a variation in fuel (e. g. usage of a green fuel), heating technique (e. g. - microwave assisted heating) can result in modification of structural, magnetic properties [14, 15].

Green nanotechnology has been described as the development of clean technologies, to minimize potential environmental, and human health risks associated with the manufacture, and use of nanotechnology products, that are more environmentally friendly throughout their lifecycle. Recent developments in nanotechnology focus on environmentally friendly, cost effective synthesizing methods (e. g. – *sol gel auto-combustion method* [15] ) via non-toxic and/or less toxic ingredients (*enhancing bio-compatibility by lowering the toxicity of the synthesized nano-particles*), and at relatively low temperatures (e. g. - below  $\sim 200$  °C) consuming less energy, and are more cost effective. Green synthesis of nanoparticles is an eco-friendly, and safe mode of synthesis of nano material includes usage of biological resources. This green approach has opened up a new era of safe nanotechnology, and has two goals: i) producing nano-materials and/or products without spoiling the environment and/or human health, and ii) producing nano-products that provide solutions to environmental problems. Sol gel auto-combustion method (*utilizing natural economical precursors e. g. - honey, aloe vera plant extract, banana peel-off, orange peel-off, ginger, cardamom seeds etc.*) can be efficiently employed to synthesize ferrite nano-particles, displaying appropriate magnetic properties [16], which are of use especially in hyperthermia applications etc. (*due to enhanced biocompatibility, lowering toxicity*) [17-19].

## POST-PREPARATION TREATMENTS

### Conventional thermal treatment

This is very critical step in the manufacturing of ferrites. At this stage the product achieves its final magnetic, and mechanical properties. As an example - sintering of manganese-zinc ferrites needs control of time, temperature and atmosphere at the each phase of the sintering cycle. Sintering starts with a gradual heating from room temperature to approximately 800 °C, as impurities, residual moisture, binders, and lubricants are burnt out of the product at this stage. The atmosphere at this stage of the sintering cycle is air. The temperature is further increased to the final sinter temperature of 1325 to 1375 °C, depending upon the composition of material. While the temperature is increasing, a non oxidizing gas, nitrogen, is introduced to reduce the oxygen content of the atmosphere. During the cool-down cycle a reduction of oxygen pressure is very critical in obtaining high quality Mn-Zn ferrites. The sintering of nickel-zinc, and lithium titanium, ferrites occurs at lower temperatures, in the range of 950 – 1250 °C, and can be sintered in an air atmosphere. During sintering the ferrite parts shrink ( $\sim 15$  to 17%) to the final

dimensions. The variation in mechanical dimensions is of the order of  $\pm 2\%$  of the basic sizes of the part. Topfer et al [20] also mention that the properties of Mn Zn ferrites, and the loss depend on the purity of raw materials, influence of the dopant and sintering process.

### **Microwave and conventional thermal treatment**

The fundamental difference between microwave sintering, and conventional sintering is in the heating mechanism. For conventional sintering, heat is generated by heating elements, and transferred to samples via radiation, conduction, and convection. In microwave assisted heating, however, the materials themselves absorb microwave energy, and then transform it into heat within their bodies [13,14]. The microwave heating presents a potential economical sintering process with shortened processing time for the materials. Microwave assisted sol gel auto combustion synthesis will be even more energy efficient (as compared to sol gel auto-combustion via conventional annealing), and is known for its high purity, simplicity, more efficient, and homogeneous heating of the reaction mixture, where synthesis time is rather short of the order of several minutes (in contrast to several hours e. g. – in ceramic method), leading to enhanced material properties [14]. Microwaves generally heat conducting ions in a solvent. By microwave heating, polar molecules (e. g. water molecules) make an effort to adjust with rapidly changing alternating electric field; heat is generated by rotation, friction, collision of molecules. This method is expected to overcome many of the shortcomings of the conventional sintering process [15]. Thus, there has been considerable interest in microwave heating for the synthesis, and processing of materials. Microwave processing has gained worldwide acceptance as a novel method for heating, and sintering a variety of materials, as it offers many advantages in terms of enhanced diffusion processes, reduced energy consumption and processing cost, very rapid heating rates, and significantly reduced processing times, decreased sintering temperatures, improved physical, and mechanical properties, simplicity, unique properties, new materials, new products, and lower environmental hazards, which are not observed in conventional processes [21-25].

### **Spark Plasma Sintering**

There is another sintering technique that is called spark plasma sintering (SPS), also known as plasma activated sintering or field-assisted sintering technique (FAST) which is an effective sintering technique that allows densification of powders or green body at a relatively lower temperature with short holding time owing to very rapid heating and cooling rates ( $\sim$  several hundred K/min.), and enables full densification within minutes. In this method, powders are placed in a graphite die, pressed uniaxially, and then heated by passing a high pulsed current through the powders and/or the die. SPS method allows to obtain high dense ceramic pellets with nanosized grains in a few minutes [26]. In SPS, mixtures typically are loaded in a cylindrical graphite die (e. g. - 10 mm inner diameter) between two pistons applying uniaxial stress. Carbon paper is generally used as separator between powder, carbon die, and pistons (*to avoid contamination of piston, die by the material which is being sintered*). The reaction, and then the sintering are carried out in neutral atmosphere (Argon) by heating the powder with a pulsed DC current under application of uniaxial stress. Typical reaction stage could be e. g. - sintering at 600 °C under a pressure of 100 MPa for 5 min [26]. Both microwave, and plasma arc sintering hold forth the promise of rapid processing as well as refinements in microstructure, and enhanced properties. Microwave sintering appears to be an attractive alternative to plasma arc sintering for large specimens, since the energy is deposited in the bulk of the material by dielectric loss mechanisms.

### **Ion irradiation**

Ion irradiation is one of the novel techniques to alter the material properties [27-29]. When ions pass through a material, they can pass on their momentum, and energy to the material. Depending on the energy of ions two regimes can be defined: via nuclear energy regime (few KeV), and electronic energy regime ( $>$  few MeV). Swift heavy ion (SHI) irradiation is known to create structural changes in spinel ferrites [30]. The magnetic properties of spinel ferrites depends on a range of factors like composition, crystal structure, crystallinity, domain structure, surface morphology. Within material ions lose their energy in two ways: (i) part of the given energy is used in embedding of ions within the samples when thickness of the sample is higher than the penetration depth of the sample, and (ii) if thickness is lower than the penetration depth of the ions then they pass through the material. The penetration depth of the ions depends on various factors e.g.- nature of ion, and its energy, charge of the ion etc. SHI

passage through materials loses their energy via electronic ( $S_e$ ) and nuclear ( $S_n$ ) energy loss. In MeV energy range  $S_e$  dominates over  $S_n$ , responsible for structural modification (*via irradiation induced defects*), would be responsible for relocation of cations among  $A$  (*Tetrahedral*),  $B$  (*Octahedral*) sites in the fcc spinel structure. SHI irradiation creates disorder in structure, produces strain, introduces point defects, remains the most prominent reason for modification of cation distribution which in-turn would affect magnetic properties [1,8].

## CHARACTERIZATION

This article utilizes respectively x-ray diffraction (XRD) and, magnetic measurements to get complementary information on structural, magnetic properties (measured by means of vibrating sample magnetometer 'VSM'), are described below.

### XRD measurements

XRD provides information on structure, various phases present in the sample under investigation. It is a handy tool, available relatively easily (as compared to transmission electron microscopy, synchrotron, neutron techniques), and provides vital information on structural properties, and in case of ferrites it also provides essential information on Neel magnetic moment, which is theoretical magnetic moment at 0 K (*obtained via cationic distribution*). Various structural parameters e. g. - degree of inversion ' $\delta$ ', oxygen positional parameter ' $u$ ', bond lengths, bond angles, dislocation density etc. play an important role in determining magnetic properties (e. g. - coercivity ' $H_c$ ', saturation magnetization ' $M_s$ ' etc.). So investigating samples via XRD is essential. XRD remains one of the best techniques to study cationic distribution in ferrites, which affects their magnetic properties. [8]. A particular composition, a specific synthesis technique, and post-preparation treatments is known to affect the properties of ferrite, which can be effectively studied through XRD studies. Magnetic properties of ferrite nanoparticles strongly depend on cationic distribution, and structural properties including grain diameter ' $D$ ' (*plays an important role in determining magnetic properties*),  $u$ ,  $\delta$ , bond lengths bond angles (helpful in determining magnetic interactions: A-A, A-B, B-B, affecting magnetic properties).

One of the very important information obtained from XRD measurements is site occupancy: i. e. presence of a specific ion, and its fraction on a particular site (A, B) in spinel structure. It is worth noting that, magnetic materials with same nominal chemical composition, even with very high phase purity, often differ noticeably from one another due to a different distribution of species or defects (i.e. ions, vacancies etc.) among the available crystallographic sites. This is particularly true for ferrimagnetic materials containing multiple sublattices. Spinel ferrites, for example, have two sublattices with parallel coupling of the magnetic moments within each sublattice and antiparallel coupling between them i. e. sublattice A, B [31]. The result is that the magnetization of the material arises from the difference in magnetization of the sublattices (A, B). Often, different species reside on each sublattice. If vacancies are found preferentially on one sublattice, or if some of the atoms on one sublattice are switched with those on the other, the magnetisation may be altered substantially [1,8,12,32]. Thus, it is very important to determine site occupancy in ferrites. X-ray diffraction (XRD) [32], neutron diffraction (ND) [33], extended X-ray absorption fine structure (EXAFS) [34], and Mössbauer spectroscopy (MS) [35] are usually employed to obtain sensible information on cation distribution in the fcc structure. ND, and EXAFS provide accurate analysis but require the access to neutron, and synchrotron sources, respectively, increasing the cost, and limiting the achievement of quick results. Also MS is a powerful tool to study environment around Fe atom, however it loses its power when non-magnetic ions are in focus. These limitations have created a need for the use of a relatively simpler but equally accurate method to obtain reliable results. In this context, XRD has established as one of the most suitable and successful tools for proper determination of cation distribution [36-38], although the effectiveness of XRD is partially limited by the similar scattering factors of some of the cations present in the spinel structure. Additionally, due to ease in availability, XRD remains one of the methods of choice for confirming presence of single expected phase as well as any secondary phases available in the sample.

It is worth noting that, by decreasing the size of ferrite nano particles, the number of atoms located at the surface noticeably increases. Thus, the surface spins become dominant in determining the magnetic properties of the whole nano particles. The atoms at the surface exhibit lower coordination numbers originating from breaking of symmetry of the lattice at the surface, and due to broken exchange bonds, resulting in the spin disorder, leading to low saturation magnetization. Observed low saturation magnetization can be explained by core shell model [38] in which the nano particles consists of a core with the normal spin arrangement, and the disordered shell, where the spins are inclined at random angles to the surface, the so called spin canting angle. Utilizing magnetic moment (Neel Magnetic moment) at A, B site (obtained by cationic distribution, calculated from XRD measurements), spin canting

angle can also be obtained. Thus, XRD provides not only vital information on structure, but also facilitates understanding magnetic properties of ferrites.

## Magnetic measurements

Vibration sample magnetometer (VSM) can be effectively used to probe magnetic properties of ferrites [1, 8, 12, 22]. Variation of temperature during VSM measurements can also be done, yields temperature dependence of magnetic properties. VSM measurements provide information on coercivity ( $H_c$ ), saturation magnetization ( $M_s$ ), Remanence ( $M_r$ ), squareness ratio ( $M_r/M_s$ ), losses, anisotropy. Thus, help in understanding the effect of: composition; a specific synthesis protocol (e. g. - sol gel auto combustion, microwave assisted sol gel auto

combustion etc.), and conditions during synthesis; e. g. - effect of pH, usage of a specific fuel like-conventional fuel: Citric acid, urea etc, green fuel etc.), and effect of post-preparation conditions (e. g. - thermal annealing, SPS, ion irradiation etc.) on the magnetic properties of spinel ferrites. Magnetic measurements provide necessary basic information on magnetic properties, and combining them with structural properties one can obtain correlation between them, which eventually can be used in perspective applications of ferrites for societal relevance.

## Preparation condition, composition, and post-preparation treatment dependence of properties

Here, representative examples of ferrite nano particles are given, depicting the effect of composition, synthesis protocol, and post preparation treatment, showing modification of structural, magnetic properties, and correlation between them.

Table 1 gives preparation condition dependence of  $a$ ,  $D$ ,  $\delta$  and  $u$ , for four different  $MgFe_2O_4$  samples, with difference in preparation conditions, described as: sample S1 - microwave assisted combustion synthesis done for 8 minutes without adjusting pH, and no further thermal treatment was used, sample S2 - sol gel auto-combustion synthesis by maintaining pH 7, and annealed at 600 °C for 3 hours, sample S3 - sol gel auto-combustion synthesis without adjusting pH, and in dry gel form and sample S4 - sol gel auto-combustion synthesis by adjusting pH to 7, and in dry gel form. All these samples are synthesized via green synthesis route, (*utilizing honey as chelating agent-fuel*), with an objective to reduce the toxicity, improved biocompatibility so the synthesized ferrite can be more suitable for their perspective applications in biomedicine e. g. - in targeted nanoparticle delivery hyperthermia. Perusal of table 1 shows that minor changes in  $a$  (range between 0.8383 - 8392 nm), detectable changes in  $D$  (range between 15.8 nm - 37.5 nm), changes in degree of inversion (range between 0.2 - 0.72), showing mixed nature of the samples, and considerable changes in  $u$  (varying between 0.3798 - 0.3827). Observed changes are ascribable to difference in cationic distribution (not shown here) accountable for changes in grain diameter, degree of inversion as well as changes in  $u$  (measure of disorder in the material). For samples S1 - S4, obtained magnetic properties show changes in magnetic softness, reflected in coercivity (range between 66.5 Oe - 112.1 Oe), significant enhancement in  $M_s$  from 6.8  $Am^2/kg$  (for sample S3) to 31  $Am^2/kg$  (for sample S1). It is worth noting that sample S1 is synthesized via microwave assisted sol gel autocombustion method, which shows highest  $M_s$  values, showing importance of microwave synthesis, in enhancing magnetic properties.

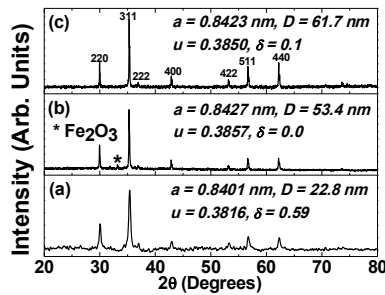


Fig. 1: XRD patterns of nanosized zinc ferrite: (a) Dry gel, (b) Ann. at 600°C/ 3h, (c) spark plasma sintered at 800°C/5 min. Lattice parameter ( $a$ ), grain diameter ( $D$ ), oxygen parameter ( $u$ ), degree of inversion ( $\delta$ ) are also shown with each XRD pattern.

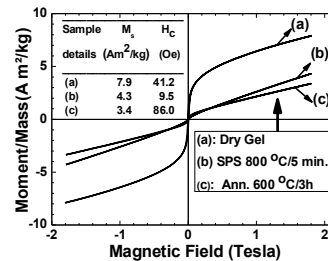


Fig. 2: Hysteresis loops of: (a) dry gel, (b) spark plasma sintered at 800°C/5 min., (c) Ann. at 600°C/3h. Saturation magnetization ( $M_s$ ), Coercivity ( $H_c$ ) are also shown in the figure.

**Table1:** Preparation condition dependence of lattice parameter ( $a$ ), Grain diameter ( $D$ ), inversion parameter ( $\delta$ ), oxygen parameter ( $u$ ).

$x$	$a$ (nm)	$D$ (nm)	$\delta$	$u$
S1	0.8384	26.0	0.72	0.3827
S2	0.8384	37.5	0.62	0.3821
S3	0.8392	16.5	0.30	0.3802
S4	0.8383	15.8	0.20	0.3798

**Table 2:** Summary of various ferrite compositions, synthesized by a specific synthesis protocol, post-preparation treatment, structural magnetic parameters, data from literature is also included (reference is shown with each sample).

Sample	Synthesis Method	Post-Preparation Treatment	$D, a_{exp}$ (nm)	$u, \delta$	Dead Layer	$M_{s(exp)}/M_{s(t)}$ ( $Am^2/kg$ )	$H_c$ (Oe)	Reference
ZnFe <sub>2</sub> O <sub>4</sub>	Sol-Gel	-	22.84,	0.3845,	-	7.8, 185.3	41.1	This work
	Auto-comb.		0.8401	0.20				
ZnFe <sub>2</sub> O <sub>4</sub>	Sol-Gel	Ann 600°C / 3h	53.37,	0.3807,	-	3.3, 86.8	86.0	This work
	Auto-comb.		0.8427	0.65				
ZnFe <sub>2</sub> O <sub>4</sub>	Sol-Gel	SPS 800°C / 5 min.	61.71,	0.3833,	-	4.3, 162.17	9.5	This work
	Auto-comb.		0.8423	0.30				
ZnFe <sub>2</sub> O <sub>4</sub> (Pristine)	Sol-Gel	-	-	-	-	26.1, -	-	[40]
ZnFe <sub>2</sub> O <sub>4</sub> (Irradiated)	Sol-Gel	100 MeV O ion	-	-	-	17.9, -	-	[40]
	Auto-comb.	5×10 <sup>13</sup>	-	-	-	-	-	
ZnFe <sub>2</sub> O <sub>4</sub> (Pristine)	Sol-Gel	-	17.4,	0.3785,	-	-	-	[41]
	Auto-comb.		0.8400	0.0				
ZnFe <sub>2</sub> O <sub>4</sub> (Irradiated)	Sol-Gel	<sup>16</sup> O <sup>6+</sup> , 80 MeV	15.7,	0.3846,	-	-	-	[41]
	Auto-comb.	1×10 <sup>11</sup> DG*	0.8423	0.85				
ZnFe <sub>2</sub> O <sub>4</sub> (Irradiated)	Sol-Gel	<sup>16</sup> O <sup>6+</sup> , 80 MeV	17.6,	0.3842,	-	-	-	[41]
	Auto-comb.	1×10 <sup>12</sup> DG*	0.8421	0.79				
ZnFe <sub>2</sub> O <sub>4</sub> (Irradiated)	Sol-Gel	<sup>16</sup> O <sup>6+</sup> , 80 MeV	16.0,	0.3836,	-	-	-	[41]
	Auto-comb.	1×10 <sup>13</sup> DG*	0.8417	0.7				
ZnFe <sub>2</sub> O <sub>4</sub> (Irradiated)	Sol-Gel	<sup>16</sup> O <sup>6+</sup> , 80 MeV	16.2,	0.3788,	-	-	-	[41]
	Auto-comb.	1×10 <sup>14</sup> DG*	0.8382	0				
MgFe <sub>2</sub> O <sub>4</sub>	Microwave-Assisted	800W power/ 8 min	26.0,	0.3827,	-	31.0, -	112.0	[14]
			0.8384	0.28				
MgFe <sub>2</sub> O <sub>4</sub> (Pristine)	Sol-Gel	<sup>28</sup> Si <sup>9+</sup> , 120 MeV	34.7,	0.3803,	4.24 nm	23.8, 44.6	106.0	[8]
	Auto-comb.	1×10 <sup>11</sup>	0.8343	0.16				
MgFe <sub>2</sub> O <sub>4</sub> (Irradiated)	Sol-Gel	Ann/450° /3h	31.0,	0.3799,	4.26 nm	15.6, 33.5	103.9	[8]
	Auto-comb.	<sup>28</sup> Si <sup>9+</sup> , 120 MeV	0.8352	0.12				
MgFe <sub>2</sub> O <sub>4</sub> (Irradiated)	Sol-Gel	Ann/450° /3h	33.3,	0.3799,	5.02 nm	8.5, 27.9	106.0	[8]
	Auto-comb.	<sup>28</sup> Si <sup>9+</sup> , 120 MeV	0.8346	0.1				
MgFe <sub>2</sub> O <sub>4</sub> (Irradiated)	Sol-Gel	Ann 450° /3h	35.0,	0.3798,	5.53 nm	4.7, 22.3	108.9	[8]
	Auto-comb.	<sup>28</sup> Si <sup>9+</sup> , 120 MeV	0.8349	0.08				
Ni <sub>0.8</sub> Zn <sub>0.2</sub> Fe <sub>2</sub> O <sub>4</sub>	Green-Synthesis	Ann.500° C/3hr.	32.7,	- , 0.82	-	52.5, 80.5	-	[14]
			0.8363					
NiFe <sub>2</sub> O <sub>4</sub> (Pristine)	Sol-Gel	-	42.8,	0.3796,	-	33.1, 49.1	157.3	[39]
	Auto-comb.		0.8335	0.01				
NiFe <sub>2</sub> O <sub>4</sub> (Irradiated)	Sol-Gel	<sup>28</sup> Si <sup>9+</sup> , 120 MeV	36.3,	0.3803,	-	20.3, 61.9	163.5	[39]
	Auto-comb.	1×10 <sup>12</sup> ions/cm <sup>2</sup>	0.8314	0.10				

\*DG - Dry Gel , Irradiation dose is given in the units of ions/cm<sup>2</sup>

Fig. 1 depicts XRD patterns of  $\text{ZnFe}_2\text{O}_4$  samples, and it can be seen very clearly that although all the samples have same composition, but thermal treatment (*dry gel, thermally annealed, spark plasma sintered samples*), show up considerable changes in lattice parameter ( $a$ ), grain diameter ( $D$ ), oxygen parameter ( $u$ ), degree of inversion ( $\delta$ ). Observed changes in  $a$ ,  $D$ ,  $u$ ,  $\delta$  (shown in figure 1) are ascribed to thermal treatment (*or no treatment for dry gel samples*) induced modification of cationic distribution (*leading to changes in degree of inversion*), grain growth, disorder, which would mirror in magnetic properties, as can be seen in figure 2, and explained later. It is worth noting that thermal annealing or no annealing has considerable effect on: grain diameter and it increases from 22.8 nm to 61.7 nm, inversion degree also changes between 0.0 to 0.59; oxygen parameter varies between 0.3816 to 0.3857 (due to migration of cations between A, B site).

Figure 2 depicts hysteresis loops of (a) dry gel, (b) spark plasma sintered at 800 °C/5 min., (c) Ann. at 600 °C/3h. Figure 2 shows that even after application of 2 Tesla magnetic field, the loops are not saturated. Values of saturation magnetization ( $M_s$ ), we represent as maximum magnetization (*as loops are not saturated*), Coercivity ( $H_c$ ) is also shown in the figure 2. Perusal of fig. 2 depicts that, for the same composition, thermal treatment results in modification of coercivity (varies between 9.5 Oe to 86.0 Oe), whereas maximum magnetization (and not saturation magnetization) range between 3.4  $\text{Am}^2/\text{kg}$  to 7.9  $\text{Am}^2/\text{kg}$ . Observed hysteresis loops,  $H_c$ ,  $M_s$  are ascribed to: thermal treatment / or no treatment induced changes in cationic distribution, modification of grain diameter, presence of a non-magnetic component (quadrupole doublet) in Mössbauer spectra (*not shown here*). Ion irradiation of  $\text{NiFe}_2\text{O}_4$  with 120 MeV  $\text{Si}^{9+}$  ions with a dose of  $1 \times 10^{12}$  ions/ $\text{cm}^2$  leads to changes in lattice parameter (as compared to pristine sample) [39], ascribed to cationic re-arrangement on A, B site, resulting in  $M_s$  reduction (from 33.01  $\text{Am}^2/\text{kg}$  to 20.32  $\text{Am}^2/\text{kg}$ ) with marginal changes in coercivity. Irradiation also causes de-clustering reducing the grain diameter from 42.8 to 36.3 nm.

More details on effect of preparation condition, composition, and post-preparation treatment on structural, magnetic properties of spinel nano ferrites are depicted in table 2, giving a detailed information on comparison between structural, magnetic properties of present work, with the data available in the literature. Perusal of table 2 demonstrates changes in structural, magnetic properties, while the preparation condition, composition, and post-preparation treatment are altered. For comparison, data from literature is also included (*reference is shown with each sample*).

## ACKNOWLEDGEMENTS

Work is partly supported by Project: CSR-IC/CRS-74/2014-15/2104. SNK acknowledges gratefully for hospitality as invited professor at ENS Universite Paris-Saclay (France), during June 2018.

## SUMMARY

Although ferrites have been investigated since long, there has been steady evolution on studies related to them, is driven by their applicability in various fields in terms of properties, needed for various applications. One of the core advantage of ferrites is shaping their structural, magnetic properties by means of parameters including a specific synthesis protocol, defined composition, post-preparation treatments, and their effect on properties can be successfully studied by complementary technique of XRD and magnetic measurements. Results on various spinel ferrite compositions are discussed, where properties can be suitably modified for their perspective applications in high frequency devices, microwave devices, bioscience.

## REFERENCES

1. S. Raghuvanshi, F. Mazaleyrat and S. N. Kane, *AIP Advances* **8**, 047804-1–11 (2018).
2. J. Smit, and H.P.J. Wijn, "Intrinsic properties of ferrites with spinel structure," in *Ferrites*, Philips' Technical Library, 1959, pp. 140-149.
3. M. S.Hossain, S. M.Hoque, S. I. Liba, and S. Choudhury, *AIP Advances* **7**, 105321-1-7 (2017).
4. S. S. Bellad, R. B. Pujar, B. K. Chougule, *Mater. Chem. and Phys.*, **52**, 166–169 (1998).
5. P. Roy, S. M. Hoque, S. I. Liba, and S. Choudhury, *AIP Advances* **8**, 105124-1-10 (2018).

6. M. Venkatesh, G. Suresh Kumar, S. Viji, S. Karthi, E.K. Girija, *Modern Electronic Materials* **2** 74–78 (2016).
7. A. Aubert, V. Loyau, F. Mazaleyrat, M. LoBue, , *J. Eur. Ceram. Soc.* **37**, 3101-3105 (2017).
8. S. Raghuvanshi S.N. Kane, et al, *J. Magn. Magn. Mater.* **471**, 521–528(2019).
9. D. Peddis, C. Cannas, A. Musinu, A. Ardu, F. Orru, D. Fiorani, S. Laureti, D. Rinaldi, G. Muscas, G. Concas, G. Piccaluga, *Chem. Mater.* **25** 2005-2013(2013).
10. A. K. Gupta; M. Gupta (June 2005) *Biomaterials.* **26** (18): 3995–4021.
11. Ramaswamy, B; Kulkarni, SD; Villar, PS; Smith, RS; Eberly, C; Araneda, RC; Depireux, DA; Shapiro, B (24 June 2015), *Nanomedicine: Nanotechnology, Biology and Medicine.* **11** (7): 1821–9.
12. P. Tiwari, R. Verma, S. N. Kane, T. Tatarchuk, F. Mazaleyrat, *Mater. Chem. Phys.* **229** (2019) 78-86.
13. H. Cui, M. Zayat, D. Levy, *J. Sol-Gel Sci. Technol.* **35**, 175 (2005).
14. P. Tiwari, S. N. Kane, R. Verma, F. Mazaleyrat , AIP Conf. Proc. (Accepted), S. Raghuvanshi, R. Verma, P. Tiwari, F. Mazaleyrat, S. N. Kane, AIP Conf. Proc. (Accepted).
15. P. Tiwari, S. N. Kane, R. Verma, F. Mazaleyrat, AIP Conf. Proc. (Accepted).
16. G. VonWhite II, P. Kerscher, R. M. Brown, J. D. Morella, W. McAllister, D. Dean and C. L. Kitchens, *J. Nanomaterials*, **2012**, 730746–1–12 (2012).
17. Das, N. Sakamoto, H. Aono, K. Shinozaki, H. Suzuki and N. Wakiya, *J. Magn. Magn. Mater.* **392**, 91 – 100 (2015).
18. A. Makridis, K. Topouridou, M. Tziomaki, D. Sakellari, K. Simeonidis, M. Angelakeris, M.P. Yavropoulou, J.G. Yovos, O. Kalogirou, *J. Mater. Chem. B* **2**, 8390-8398(2014).
19. Y. Oh, N. Lee, H.W. Kang, J. Oh, , *Nanotechnology* **27**, 115101-1-21 (2016).
20. J. Topfer, A. Angermann , *Mater. Chem. Phys.* **129**, (1) 337-342 (2011).
21. R. Valenzuela, *Magnetic Ceramics*, Cambridge University Press, 2005., J.L. Dorman, D. Fiorani, Magnetic properties of fine particles, North Holland, Amsterdam (1992), D. Peddis, C. Cannas, A. Musinu, A. Ardu, F. Orru, D. Fiorani, S. Laureti, D. Rinaldi, G. Muscas, G. Concas, G. Piccaluga, *Chem. Mater.* **25**, 2005(2013).
22. M. Satalkar, S. N. Kane, A. Ghosh, N. Ghodke, G. Barrera, F. Celegato, M. Coisson, P. Tibert, F. Vinai, *J. Alloys and Comp.* **615**, S313-S316(2014).
23. S. Panchal, S. Raghuvanshi, K. Gehlot, F. Mazaleyrat, S. N. Kane, *AIP Adv.* **6**, 055930-1-6(2016).
24. Ming-Ru Syue, Fu-Jin Wei, Chan-Shin Chou, and Chao-Ming Fu, *J. Appl. Phys* **109** (2011) 07A324-1-3.
25. M. A. Gabaln, Y.M.Al Angari, *J. Magn. Magn. Mater.* **322**, 3159-3165 (2010).
26. V. Loyau, V. Morin, G. Chaplier, M. LoBue, and F. Mazaleyrat, *Journal of Applied Physics* **117**, 184102 -1 15 (2015).
27. B. Kaur, M. Bhat, F. Licci, R. Kumar, S.D. Kulkarni, P.A. Joy, K.K. Bamzai, P.N. Kotru, *J. Magn. Magn. Mater.* **305**, 392–402 (2006).
28. J.P. Singh, G. Dixit, R.C. Srivastava, H. Kumar, H.M. Agrawal, R. Kumar, *J. Magn. Magn. Mater.* **324**, 3306–3312 (2012).
29. D.K. Avasthi, G K Mehta, *Swift Heavy Ions for Mater. Eng. and Nanostructuring*, Springer ser., 2011.
30. R. Kumar, S.K. Sharma, A. Dogra, V.V.S. Kumar, S.N. Dolia, A. Gupta, M. Knobel, M. Singh, *Hyperfine Interactions* **160**, 143–156(2005).
31. M. A. Willard, L. K. Kurihara, E. E. Carpenter, S. Calvin and V. G. Harris, *Inter. Mater. Rev.* **49**, 125-170 (2004).
32. L. Gastaldi, A. Lapicciarella, *J. Solid State Chem.* **30**, 223–229 (1979).
33. D. Peddis, N. Yaacoub, M. Ferretti, A. Martinelli, G. Piccaluga, A. Musinu, C. Cannas, G. Navarra, J.M. Greneche, D. Fiorani, , *J. Phys. Condens. Matter.* **23** 426004-1-8(2011).
34. V.G. Harris, N.C. Koon, C.M. Williams, Q. Zhang, M. Abe, J.P. Kirkland, *Appl. Phys. Lett.* **68**, 2082–2084 (1996).
35. S.P. Yadav, S.S. Shinde, P. Bhatt, S.S.Meena, K.Y. Rajpure, *J. Alloys Comp.* **646**, 550–556 (2015).
36. D.V. Kurmude, R.S. Barkule, A.V. Raut, D.R. Shengule, K.M. Jadhav, *J. Supercond. Nov. Magn.* **27**, 547–553 (2013).
37. A. Najafi Birgani, M. Niyafar, A. Hasanpour, *J. Magn. Magn. Mater.* **374**, 179–181 (2015).
38. Coey JMD. *Phys Rev Lett* **27**, 1140-1142 (1970).
39. R. Sharma, S. Raghuvanshi, M. Satalkar, S. N. Kane, T. R. Tatarchuk, F. Mazaleyrat, AIP Conference Proceedings **1953** 030117-1-5 (2018).
40. J. P. Singh, R. C. Srivastava, H. M. Agrawal, R. Kumar, V. R. Reddy, A. Gupta, *J Magn. Magn. Mater.* **322**, 1701–1705 (2010).
41. M. Satalkar, S. N. Kane, S. Raghuvanshi, AIP Conf. Proc. **1953** 030069-1–4 (2018).